JOURNAL OF MATERIALS SCIENCE **35** (2000) 3631–3639

Oxidation behavior of hot isostatically pressed silicon nitride containing Y_2O_3

HONGSANG RHO, N. L. HECHT*, G. A. GRAVES
University of Dayton Research Institute, Dayton, Ohio 45469-0172, USA
E-mail: hechtj@flyernet.udayton.edu

Oxidation in the presence of air and water vapor at high temperatures was studied for Si_3N_4 ceramics containing Y_2O_3 and Al_2O_3 as sintering aids. The test environments for this study consisted of air with 0, ~1.2, and 6.4 v/o H_2O at temperatures from 1000°C to 1350°C. The oxidation exposure times were up to 500 hours. The presence of water vapor enhances oxidation and crystallization of the oxidation phases. Weight loss was observed for the oxidation in air or dry air because of Na contamination during fabrication. The effect of applied stress on the growth of the oxide scale is minimal, however, the applied stress resulted in deeper penetration of oxygen and pit formation in the oxide phase.

1. Introduction

Silicon nitride (Si_3N_4) and silicon carbide (SiC) ceramics have been identified for a number of high temperature applications. Si_3N_4 ceramics do not exhibit the same high microstructural stability and high temperature creep resistance as exhibited by SiC ceramics, but they have excellent strength, fracture toughness and thermal shock resistance, good oxidation resistance, low weight and low thermal expansion.

Although these non-oxide ceramics are good candidates for high temperature structural applications, the specific silicon based ceramics will behave differently when used at elevated temperature under stress, especially in oxidizing or corrosive environments. These ceramics are susceptible to slow crack growth, creep damage and stress corrosion. If the reliability of a component is estimated, without considering time dependent changes in the material under service conditions during prolonged loading, life predictions will not accurately reflect actual performance. Therefore, a thorough investigation of time dependent behavior at high temperatures under stress is necessary for reliability analysis.

Recent efforts to improve thermal efficiency in power generating gas turbines have focused on increasing the turbine inlet temperature by innovative turbine cooling techniques or by the use of high temperature materials [1]. If all components are replaced with ceramics, less or no cooling air would be necessary. However, only components which are exposed to high temperature and low stress are being considered for replacement with ceramics. Therefore, the use of thermal management is still necessary. Currently steam cooling is of considerable interest as an alternative method to air cooling. It is more efficient than air cooling because heat loss from the turbine gas stream would be partially recovered in a combined cycle. There are two kinds of steam cooling: (1) closed circuit and (2) open circuit. Open circuit steam cooling is ideal for use in steam injection gas turbines [1]. In open circuit steam cooling, the ceramic components would have greater steam exposure. In land based gas turbines combustion environments also affect the performance of ceramic components [2].

To assess the effect of a steam environment (water content and temperature) on grain boundary oxidation, weight gain measurements in combination with oxide thickness measurement (by AES depth profiling) were performed at three different temperatures and/or three different water contents. To assess the effect of stress on oxidation, specimens were oxidized under an applied stress and the thickness of the oxide scale was measured. The mechanical behavior of these ceramics in the presence of water vapor at elevated temperatures is discussed in a recent article [3].

2. Experimental procedure

2.1. Materials

Norton NT 164 (Si_3N_4 ceramics) were used in the oxidation study. It is known that 4 wt% Y_2O_3 was used as the densification aid for NT 164. The manufacturer also indicated that NT 164 was heat treated after machining. Two batches of NT 164 specimens were used in the oxidation experiments. The compositions of the two batches are the same, but the heat treatment after machining was different. The two batches of NT 164 are designated as NT 164-95 (1995 vintage) and NT 164-93 (1993 vintage). The NT 164-93 was heat treated at 1400°C for 5 hours. The heat treatment specifics used

* Author to whom all correspondence should be addressed.

for NT 164-95, although different, was not disclosed. Stress oxidation tests were performed on NT 164-93. Thin specimens of NT 164-93 were machined from NT 164-93 tensile specimens tested at room temperature. The thin NT 164-93 specimens were polished on the both surfaces on which maximum tensile and compressive stress was applied.

2.2. Oxidation tests

A 1600°C furnace (Theta Industries, Port Washington, NY) with an Al_2O_3 split tube was used for these oxidation experiments. Specimens were placed on a SiC support located in the hot zone of the furnace. The bars were exposed at 1000°, 1150°, 1350°C in air for 100 hours and also exposed at 1350°C in dry air, air, and wet air (air with 6.4 v/o H_2O) for up to 500 hours. After the specimens were exposed for the selected period of time, they were removed from the furnace to be characterized. The dry air was prepared by passing it through two $CaCl_2$ drying traps at a flow rate of 1.2 ml/min. Wet air was generated using an apparatus developed by Komeya *et al*. [4].

2.3. Stress oxidation tests

To investigate the effect of stress on oxidation behavior, specimens were exposed for 50 hours at 1320°C under the application of a 3 point bending stress. The major span of the bend fixture was 40 mm. A maximum stress of 200 MPa was applied to the center of specimens. To measure the thickness of the oxide that formed on the exposed specimens, the tensile and compression surfaces were partially masked with wax and soaked in 52% HF solution for 30 minutes at room temperature. The partially etched specimens was rinsed with distilled water several times and then neutralized with a concentrated KCO_3 solution for 20 minutes. The coated wax was removed with hexene solution in the ultrasonic cleaner. The step height was measured with a profilometer.

2.4. Analysis

The mass change due to oxidation was measured using a microbalance with a sensitivity of 10^{-7} g. The oxidation products and oxidation affected layers were examined using optical microscope (OM, Nikon Epiphot, Nikon Co., Japan) and a field emission scanning electron microscope (Leica Cambridge Stereoscan 360 FE, Leica Cambridge Co., Cambridge, U.K.). To prevent charging on the specimens, a carbon coating was used to examine the morphology and to conduct the elemental analysis. A Gold-Palladium coating was used only for the topographical analysis.

The chemical nature of the oxide was determined by Auger Electron Spectroscopy (AES, Varion Model 981-2707 AES, Palo Alto, CA) depth profiling. On each specimen, the area of interest was sputtered prior to analysis to remove contamination. Specimens with surface oxide layers (<1 μm thick) were analyzed using argon ion sputtering with a Varian Model 981-2043 ion gun operating at 2 kV. The sputter rate was determined to be 10 nm/min as compared with a SiO_2/Si standard whose oxide thickness had been determined by ellipsometry. Specimens with thicker oxides were analyzed using AES and crater-edge profiling. The crater was generated by grinding the oxide surface with a rotating stainless steel ball coated with diamond paste (0.1 and 1 μm). The AES crater edge profile was obtained by using a single line scan across the crater while collecting spectra for the elements of interest. The electron beam was focused to a spot $\sim$10 μm in diameter to generate the crater edge profiles. Further details of the crater-edge profiling technique have been described elsewhere [5].

3. Results and discussions

3.1. Oxidation tests

3.1.1. Weight gain measurement

The as received NT 164 specimens have an oxide layer because of heat treatments after machining. For the NT 164-93 specimen the oxide crust (defined as the zone of complete oxidation) was 0.5 μm thick and the oxide subscale (defined as the intersection of N and O profiles) was 1.5 μm thick, as determined by sputtering and AES depth profiling. NT 164-95 specimen had a thicker oxide crust (0.7 μm) than the NT 164-93 specimen, but the oxide subscale was thinner (1.2 μm).

The oxidation behavior at 1350°C for the NT 164 Si_3N_4 was characterized by measuring weight change per unit area as a function of water content in the test environment. The results of the measurements obtained are presented in Fig. 1. The water content in air was assumed to have an average value of 1.2 vol%. From the data obtained it is observed that the oxidation rate was enhanced as the water content was increased. NT 164-93 exposed in dry air showed weight loss during the first 100 hours. Three possible causes for this weight loss are: (1) diffusion outward of excess oxygen dissolved at the oxide layer and grain boundary during heat treatments, (2) escape of nitrogen trapped in the specimen, and (3) volatilization of reactants and/or products. The manufacturer of NT 164-93 has indicated that this materials was heat treated at 1400°C after hot isostatic pressing (HIP). Heat treatment at 1400°C would exclude the second cause since the

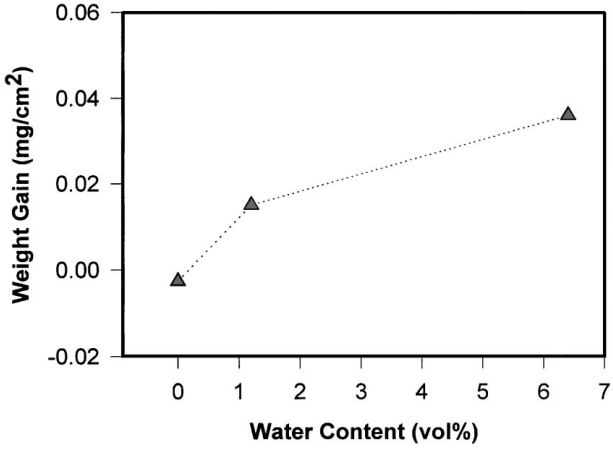

Figure 1 Weight changes of NT 164-93 exposed at 1350°C for 100 hours as functions of water content.

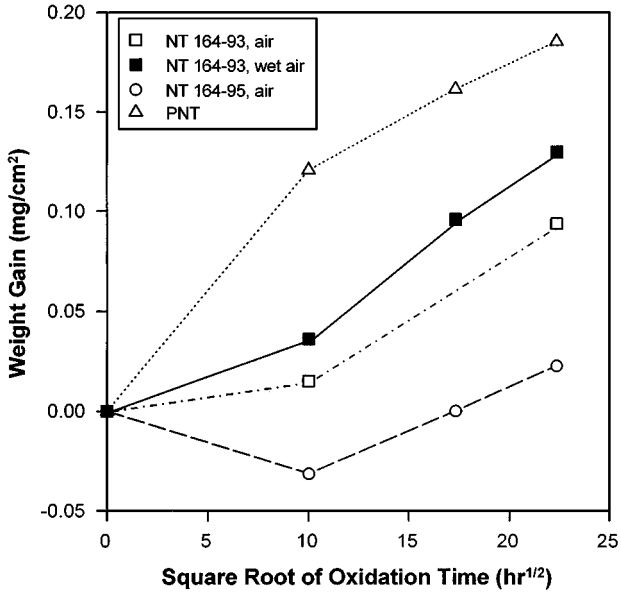

Figure 2 Parabolic fitting of weight gain for NT 164-93, NT 164-95, and polished NT 164-93 (PNT) at 1350°C in air and in wet air.

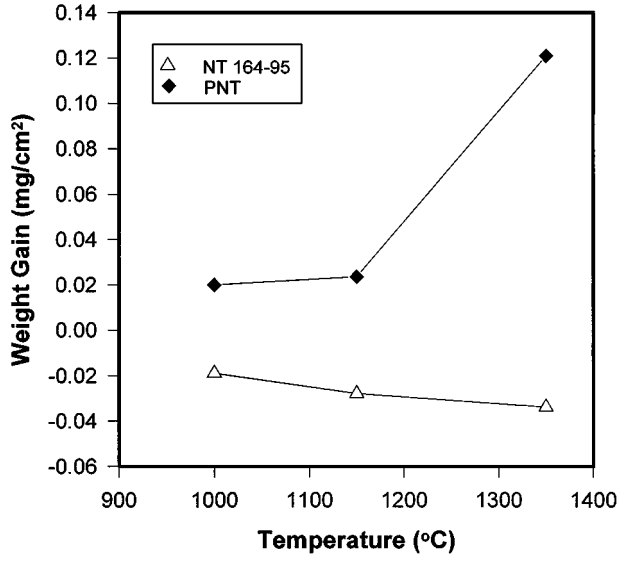

Figure 3 Weight changes of NT 164 as a function of temperature.

oxidation temperature is lower than the heat treatment temperature.

Weight gains were plotted as a function of the square root of oxidation time (up to 500 hours) in Fig. 2 to determine if the kinetic rate is parabolic. NT 164-93 displayed deviation from the parabolic rate law for the first 100 hour exposure both in air and in wet air. This phenomena seems to be related to similar weight loss observed in dry air during the first 100 hour exposure. The weight gain in wet air was double that in air for the 100 hour exposure, but the difference diminished with exposure time. The overall parabolic rate constant for NT 164-93 in wet air oxidation was 50% greater than for air oxidation. The NT 164-95 showed significant weight loss for the first 100 hours, which was followed by weight gain. NT 164-93 showed less weight loss than NT 164-95 suggesting that weight loss depends on heat treatment conditions. PNT (NT 164-93 without post heat treatment) also deviated from the parabolic rate. During the first 100 hours the PNT experienced rapid oxidation during initial exposure followed by slow oxidation. Similar deviations from the parabolic kinetic law for Si_3N_4 ceramics was observed by Chen *et al*. [6]. The composition of the Si_3N_4 ceramics used in their study was similar to that of NT 164. They observed that there was an initial rapid weight gain followed by little weight change during the 20–80 hour oxidation period, and then a weight gain after an extended oxidation period.

Oxidation tests for NT 164-95 and PNT in air were also conducted at 1000 and 1150°C for 100 hours. The weight change vs. temperature for this oxidation test is plotted in Fig. 3. NT 164-95 showed decreased weight loss as the temperature decreased. Since there is the possibility that both weight loss and weight gain processes occur during the 100 hour exposure, it is not possible to calculate real weight loss. It can, nevertheless, be concluded that the process of weight loss is highly dependent on the dominate diffusion process at the exposure temperatures. PNT (NT 164-93 with the surface polished) showed a small temperature dependence between 1000 and 1150°C. The temperature dependence for oxidation increased significantly above 1150°C.

3.1.2. Microstructure analysis

SEM micrographs of the cross sections of oxide scales of NT 164-93 specimens oxidized at 1350°C for 500 hours in air and in wet air are shown in Fig. 4. A much thicker oxide crust was formed in wet air than in air. Equiaxed cristabolite grains are clearly seen in Fig. 4b. To investigate the oxidation zone in more detail, ball crating, optical microscope (OM) and scanning electron microscope (SEM) analysis were used. SEM pictures (secondary and backscattered electron) and OM pictures of the ball crater of NT 164-93 oxidized in wet air for 500 are presented in Fig. 5. Fig. 6 shows the SEM pictures for each of the regions labeled in Fig. 5. Cracking of the oxide layer was observed but spalling of the oxide was not observed. Acicular crystals which formed on the outer layer of the oxide were embedded to some depth followed by a Y depletion zone. The number of crystals was decreased and the size and aspect ratio of the individual crystals was larger as the oxidation process proceeded. Based on the EDS analysis, these acicular crystals are rich in Y and Si, and are presumed to be Yttria silicates ($Y_2Si_2O_7$). The matrix was predominantly silicon oxide with some Al impurities. These Al impurities seemed to be contamination from the alumina tube in the theta furnace. The dark color crystals in the matrix appeared to be cristobalite. In the picture of the oxide crust (Fig. 5b), two layers are observed. Higher magnifications of the black band region are shown in Fig. 6(2). Cristobalites surrounded by a glass phase were observed, however, more complex silicate crystals were not observed. At the deeper region in the black band, the glass phase surrounding the SiO_2 crystals is reduced and silicate crystals are observed. At the boundary between the oxide crust and the reaction zone a porous layer with many tiny white crystals is observed. This porous layer seems to be related to the weight loss in the early stage of

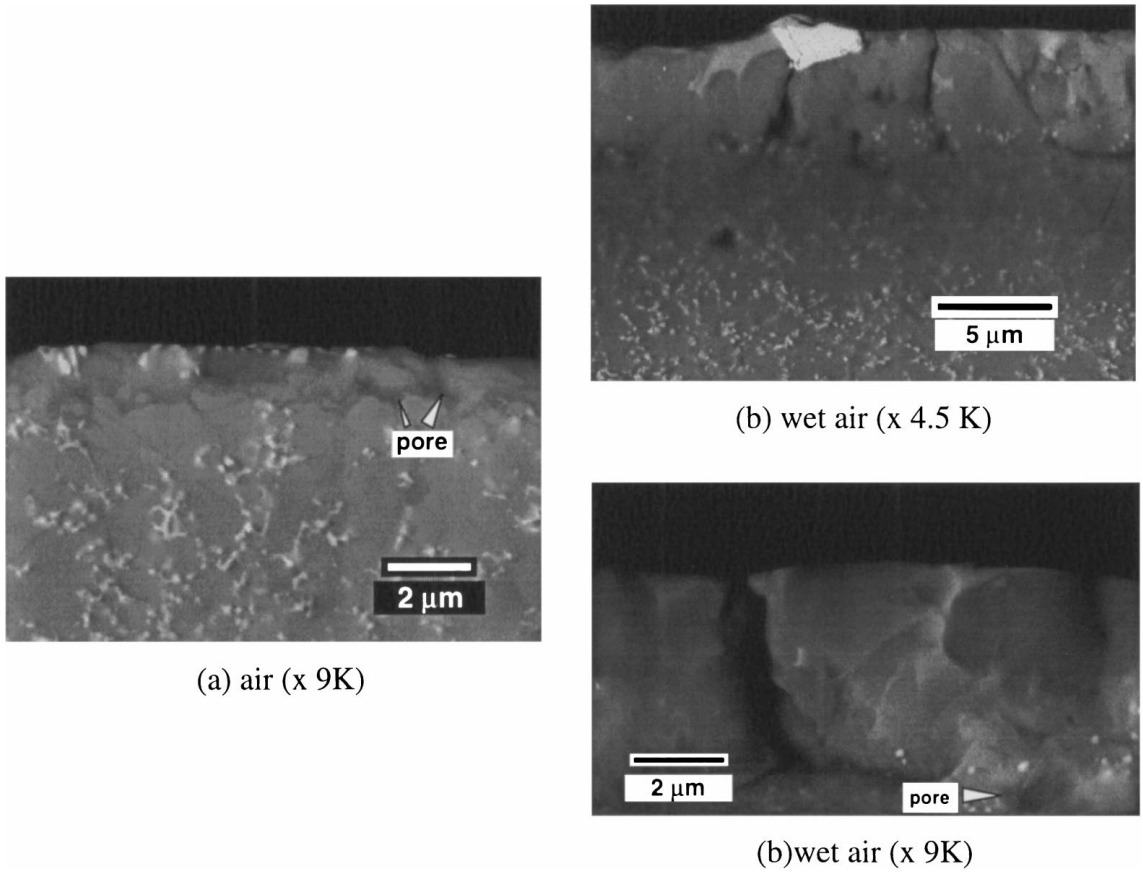

Figure 4 SEM micrographs of the cross sections of oxide scales of NT 164-93 oxidized at 1350°C for 500 hours (a) in air and (b) in wet air.

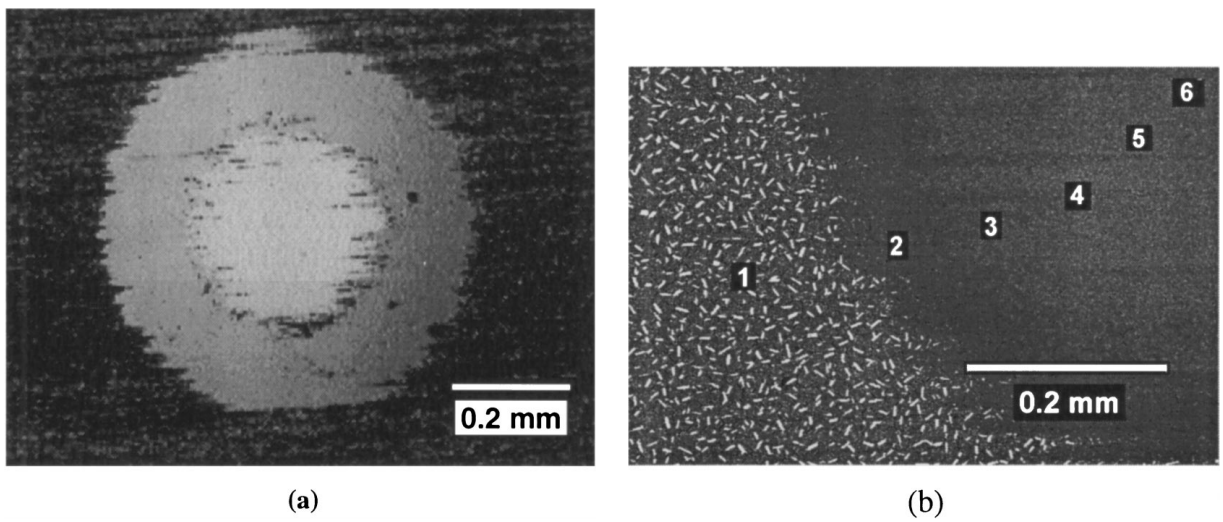

Figure 5 (a) optical microscope photo of ball crater, (b) back scattered electron SEM photo of one quarter of the ball crater on NT 164-93 specimen oxidized at 1350°C in wet air for 500 hours where the regions are denoted as 1-surface, 2-1st oxide crust, 3-2nd oxide crust, 4-porous layer, 5-reaction zone, and 6-substrate.

oxidation. The pores became smaller as oxidation proceeded. Individual oxidized grains could be seen inside the pores [Fig. 6(4)]. Maeda *et al*. [7] suggested that the pores generated by crystallization of cristobalite is the reason for increased oxidation in the presence of water vapor. Those kinds of pores were not observed in this study. The pores observed in this study seem to form in the early stage of oxidation. The major difference between the reaction zone and the substrate was higher porosity in the reaction zone of the NT 164-93.

NT 164-93 oxidized at 1350°C in air for 500 hours showed quite a different morphology than that observed for NT 164-93 oxidized in wet air. Fig. 7 shows the morphological difference of the surfaces of those specimens. The number and size of the silicate crystals on the surface of the specimen oxidized for 500 hours in air was much smaller than the yttrium silicate crystals observed on the specimen oxidized for 500 hours in wet air. It was also observed that the yttrium silicates are distributed evenly along the depth of the oxide

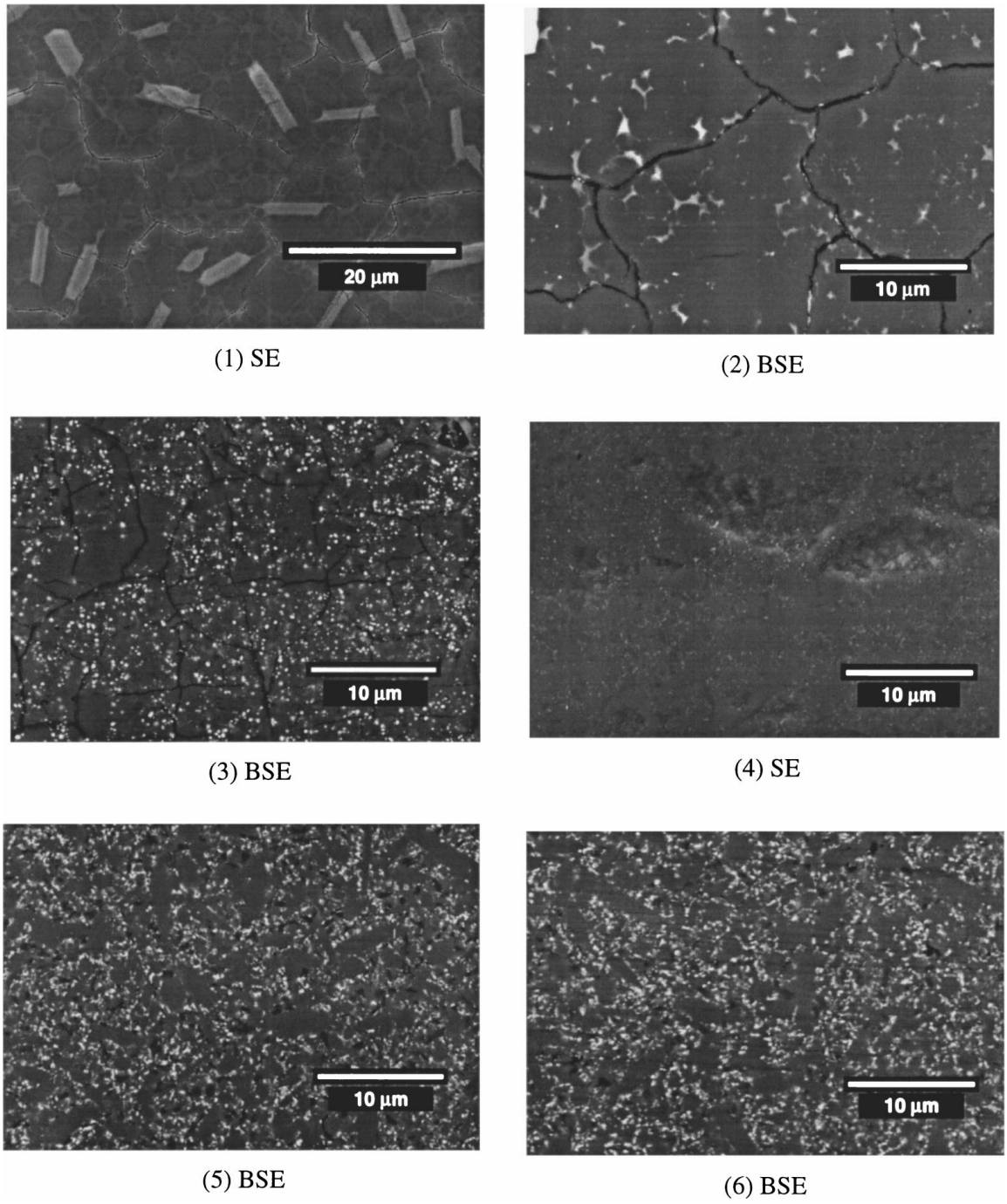

Figure 6 Enlarged regions of 1-surface, 2-black band, 3-oxide crust below black band, 4-porous layer, 5-reaction zone, and 6-substrate as labeled in Fig. 5.

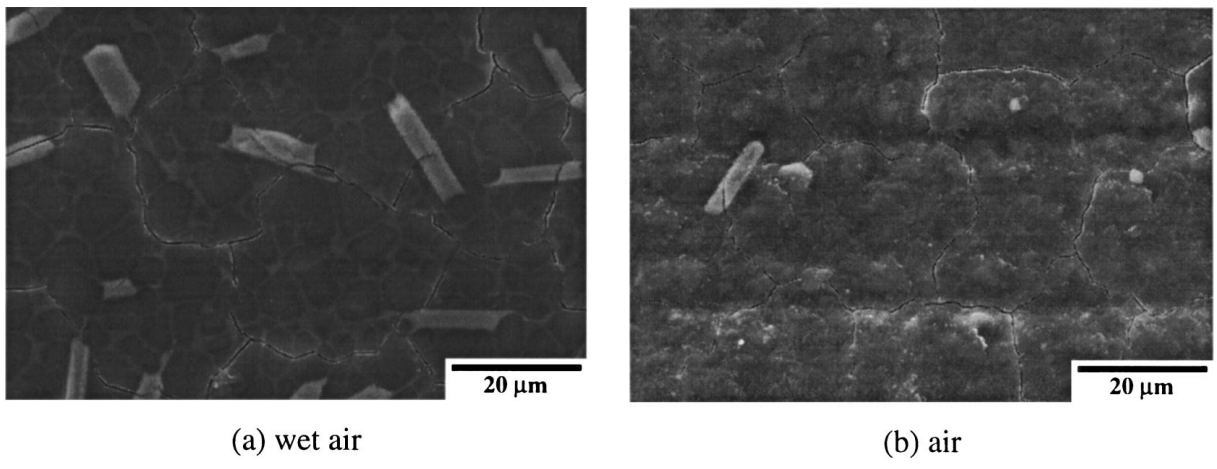

Figure 7 Mophological difference between the specimens oxidized at 1350°C for 500 hours in wet air and in air.

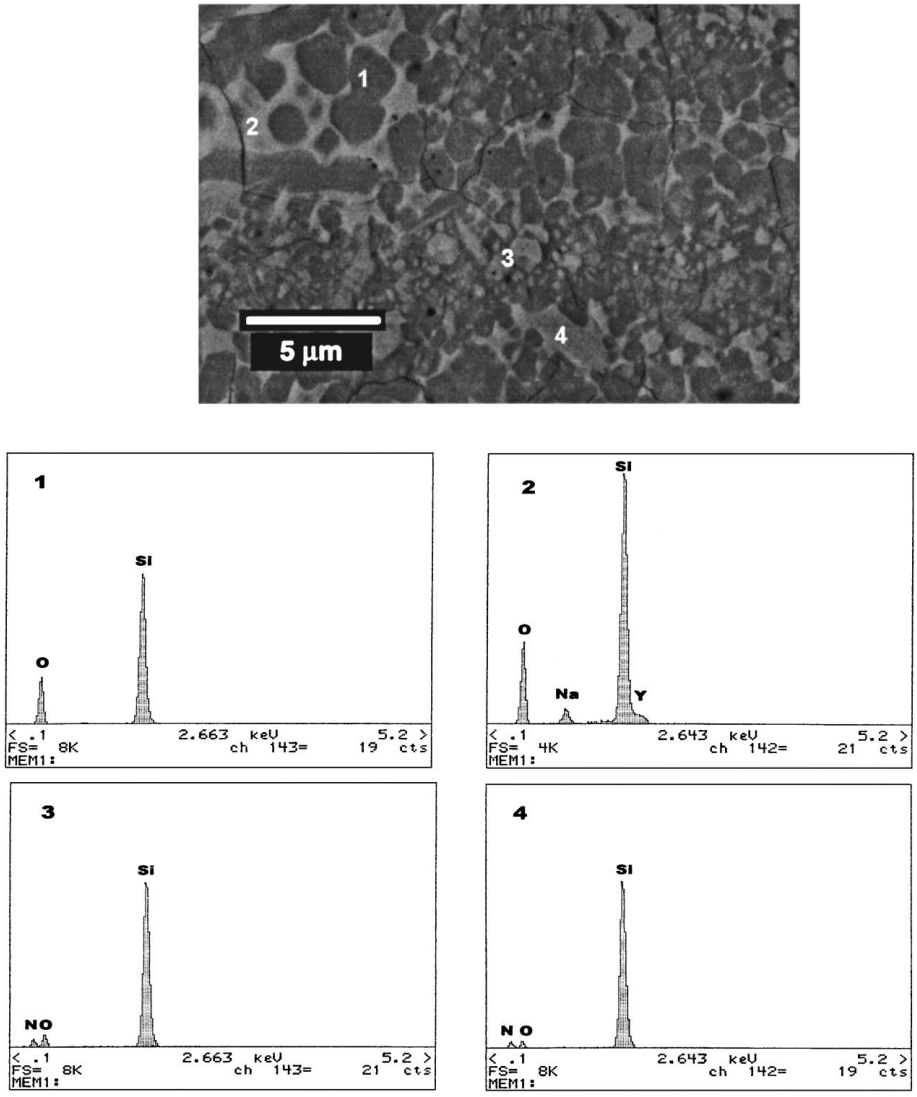

Figure 8 Surface morphology of as received NT 164-95 specimen and EDX analysis of marked regions.

layer in air oxidation. Another difference between those specimens was the pore morphology at the interface of the oxide crust and reaction zone. Bigger pores were observed in the specimen oxidized in air than the specimen oxidized in wet air. From these observations, it is conjectured that the presence of water vapor accelerated both crystallization and crystal growth and it also was more effective in flaw healing.

To investigate the weight loss of NT 164-95 in the passive region, SEM pictures were taken on the surface of an as-received specimen. The surface morphology and EDX patterns of selected locations are shown in Fig. 8. Heterogeneous oxidation was observed on the surface of the as-received specimen. The regions marked by 1 and 2 exhibited greater oxidation than those marked by 3 and 4. The Na contamination is believed to come from the glass encapsulation used in the hot isostatic pressing process. This contamination seems to be related to the weight loss observed in the oxidation test. Jacobson *et al*. [8] illustrated that a small amount of Na_2O would be expected to form a low melting sodium silicate [$Na_2O{\cdot}x(SiO_2)$]. The lowest melting point of sodium silicate ($Na_2O{\cdot}2SiO_2$) is 874°C. Therefore, it is conjectured that the weight loss measured for NT 164-95 is caused by volatilization of the glassy phase in the grain boundary which was contaminated by impurities such as Na or K ions (from glass encapsulation).

3.1.3. AES depth profiling

The oxygen profiles from the AES depth analysis on the ball crater for as received NT 164-93 and those specimens oxidized in wet air for 100 and 500 hours are plotted in Fig. 9. The thickness of the oxide crust and reaction layer measured with AES depth profiles is shown in Table I. During the first 100 hours, oxidation through the grain boundary was enhanced. When oxidation was extended to 500 hours, bulk oxidation was quite dominant. Therefore, X_{rx}/X_{ox} (the ratio of subscale thickness to oxide thickness) was reduced from

TABLE I Thickness of oxidation products formed at 1350°C measured from AES depth profile

	Oxide crust	Point of intersection (N&O profiles)
Air, 500 hours	2.43 μm	3.7 μm
Wet air, 100 hours	1.0 μm	2.2 μm
Wet air, 500 hours	5.3 μm	6.3 μm

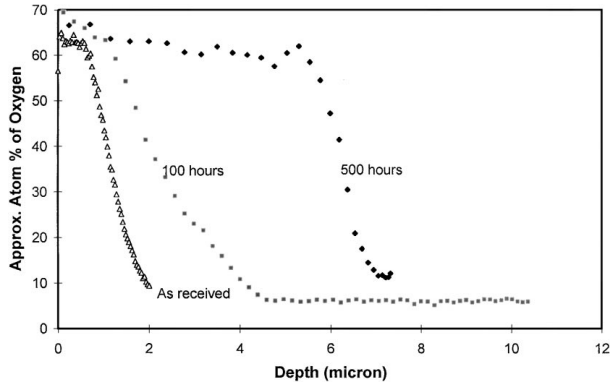

Figure 9 Oxygen profiles for as received NT 164-93 and those specimens oxidized at 1350°C in wet air for 100 and 500 hours.

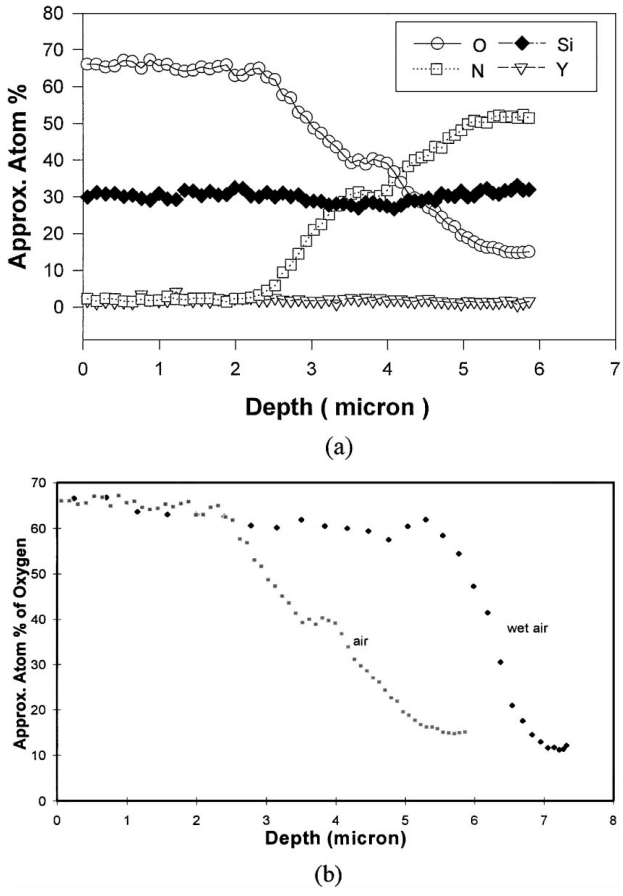

Figure 10 (a) AES depth profile of NT 164-93 specimen exposed at 1350°C in air for 500 hours and (b) comparison of oxygen profiles for specimens oxidized in air and in wet air for 500 hours.

3.7 to 0.5. The change of oxidation behavior with oxidation time may be due to a change in the nature of the oxide crust produced and the grain boundary phase. Water vapor usually accelerates the crystallization of the glass phases. Fig. 10 shows the AES depth profile of NT 164-93 after exposure in air for 500 hours and the comparison of oxygen profiles for specimens oxidized in air and in wet air. The plateau in the oxygen at the oxide/substrate interface on the specimen oxidized in air could be an artifact due to superposition of the surface roughness on the profile. Excluding that zone, the thickness of the oxide crust and subscale was 2.3 μm and 3 μm, respectively. For oxidation in air, X_{rx}/X_{ox} shows little change after the 500 hours of oxidation. The difference in the surface morphologies between NT 164-93 oxidized in air and oxidized in wet air is that the crystal nucleation and growth of yttrium silicate and cristobalite was enhanced in wet air. A layer of continuous crystalline phase with low concentration of yttria was found between the surface and the porous layer. The trend observed in the oxidation behavior for NT 164-93 in the two different test environments were similar to the previous work [9] for Si_3N_4 ceramics containing Yb_2O_3 as a sintering aid. During the oxidation in wet air, dissolution of Si_3N_4 grains is fast but diffusion of oxygen through the grain boundary becomes the rate controlling step as the oxidation time increases. It was also concluded that cristobalite in the oxide layer does not provide an efficient diffusion barrier for oxygen since there is no change in the rate of oxide crust formation. However, the dissolution of Si_3N_4 grains is the rate controlling step in air oxidation. The conclusion reported by Backhaus-Ricoult *et al.*'s [10] for the rate controlling step for air oxidation of Si_3N_4 was the same as those obtained in this study.

3.2. Stress oxidation tests

The results of the investigation of the effects of applied stress on the oxidation behavior of NT 164 at 1320°C in air and wet air are compiled in Table II. Step height produced by etching the oxidized specimens was measured by profilometer. As shown in Table II, stress appeared to have little effect on the growth of the oxide scale. Only a small difference of the penetration depth of oxygen was observed for NT 164 between the non-stressed zone and the tensile stressed zone (Fig. 11). However, as shown in Table II the effect of water vapor almost doubled the thickness of the oxide crust. Although the presence of tensile and compressive stresses did not affect the growth of the oxide scale, the stress did appear to generate pits in the oxide scale. Early stage of pit formation and the crystallite structure that surrounds the pit is shown in Fig. 12. The cause of pit formation on the oxide surface in the presence of stress has not been fully clarified. Lange [11] explained that the presence of Fe caused pitting in Si_3N_4 materials during oxidation. Gogotsi and Grathwohl [12] also proposed that pitting is generally associated with local composition inhomogeneities such as iron inclusions, leading to the formation of a low melting eutectic liquid phase at the early stages of oxidation and to dissolution of Si_3N_4 in

TABLE II The results of stress oxidation for NT 164 at 1320°C in air and wet air

	Non stress	Low stress	High stress
1. Oxide thickness in air			
Tension surface	523 nm	519 nm	512 nm
	Std. Dev. 8	Std. Dev. 22	Std. Dev. 23
Compression surface	498 nm	488 nm	486 nm
	Std. Dev. 15	Std. Dev. 18	Std. Dev. 29
2. Oxide thickness in wet air			
Tension surface (NT 164)	1.0 μm Std. Dev. 0.04	1.02 μm Std. Dev. 0.07	0.99 μm Std. Dev. 0.04

this liquid. Local composition inhomogeneities causing pit formation does not seem to be confined to Fe inclusions. Satellite rod like crystals were found by EDX to be rich in Y ions which are presumed to be yttrium silicate. White phases within the core surrounded by yttrium silicate crystals in Fig. 12 were determined to be rich in Al, Y, and Fe by EDX. Localized grain boundary attack and enhanced cation migration occurred in this region because high Y, Al, and Fe contents lowered the viscosity and led to a more open structure of the liquid phase in grain boundaries. Volatilization of the glass phase also occurred at the core. It is interesting to note that oxidation pitting is less severe in wet air than in air, possibly because of a flaw healing process in the presence of water.

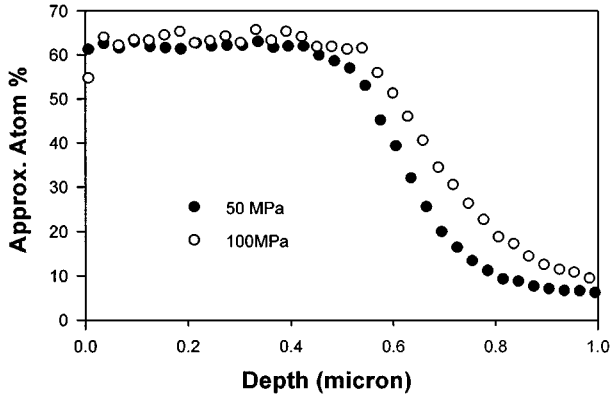

Figure 11 The effect of tensile stress on the penetration of oxygen for NT 164 stress-oxidized at 1320°C for 50 hours.

4. Summary of findings

1) Weight loss was observed for the oxidation of NT 164-95 in air and NT 164-93 in dry air due to the presence of Na contamination from the fabrication process.

2) The presence of water vapor accelerated oxidation and crystallization of oxide phases in the scale.

3) AES depth profile across the ball crater ground in the oxidized surface showed that the shape of the oxygen concentration profile changed as a function of time. Based on the AES profile data, it is proposed that dissolution of Si_3N_4 grains is the rate controlling

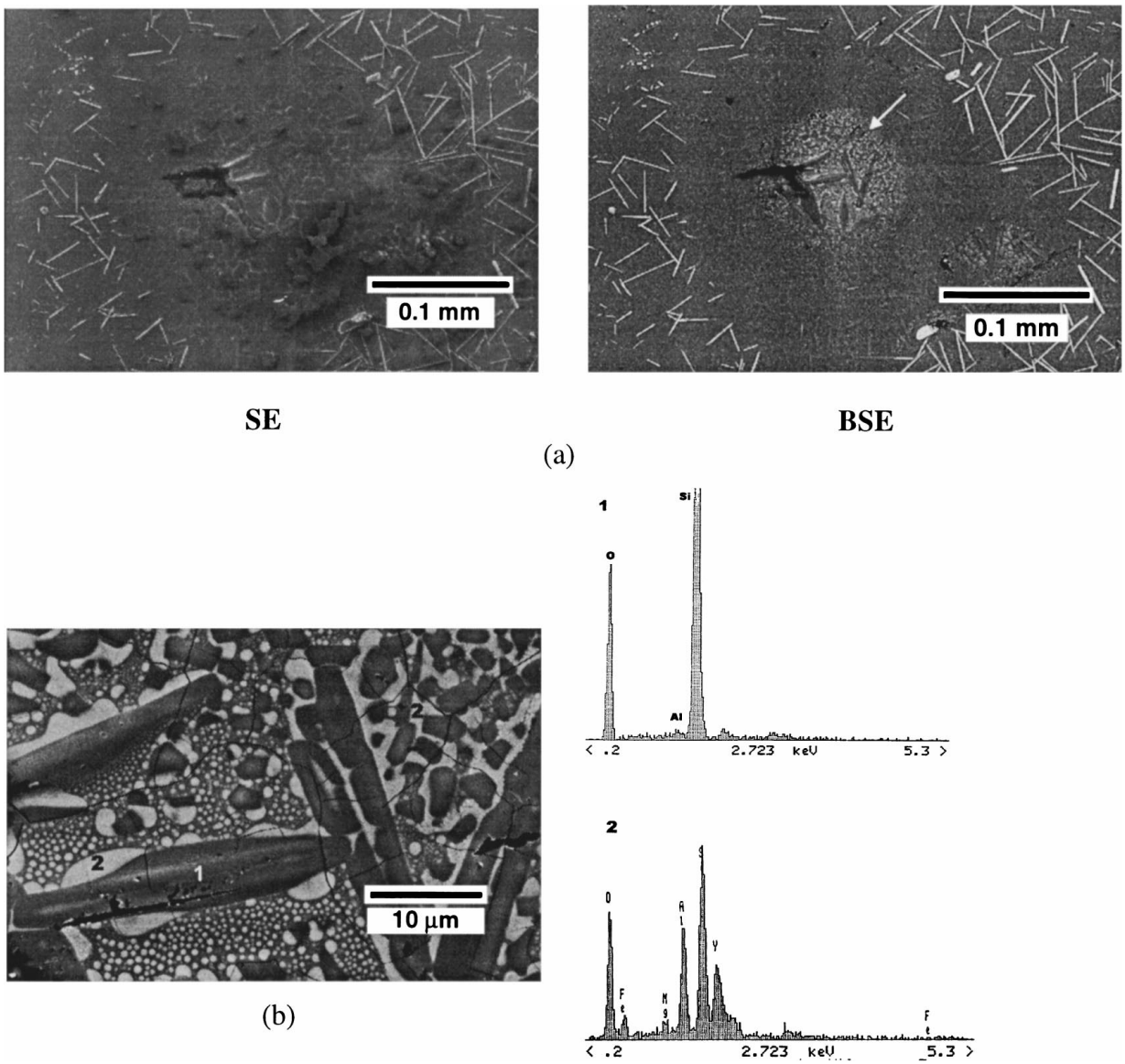

Figure 12 Pit formation in a PNT specimen stress oxidized at 1320°C in air; (a) early stage of oxidation pit, and (b) high magnification of the area marked by a white arrow and EDX analysis on the areas denoted as 1 and 2.

step in air, while diffusion of oxygen through the grain boundary is the rate controlling step in wet air.

4) Oxidation of NT 164 Si_3N_4 ceramics does not proceed layer by layer. Water vapor accelerates the dissolution reaction of Si_3N_4 grains. Grain boundary diffusion is more predominant in air as the oxidation temperature decreases.

5) The effect of stress on oxidation was minimal. Only slightly enhanced grain boundary oxidation was observed. The oxidation pits observed on the NT 164 specimens were more frequent in air than in wet air.

References

1. R. S. HOLCOMB, unpublished work.
2. N. S. JACOBSON, *J. Amer. Ceram. Soc.* **76**(1) (1993) 3.
3. H. RHO, N. L. HECHT and G. A. GRAVES, *J. Mater. Sci.* **35** (2000) 3631.
4. K. KOMEYA, Y. HARUNA, T. MEGURO, T. KAMEDA and M. ASAYAMA, *ibid.* **27** (1992) 5727.
5. J. M. WALLS, I. K. BROWN and D. D. HALL, *Applications of Surface Science* **15** (1983) 93.
6. CHEN, J. SJOGER, O. LINDQVIST, C. O'MEARA and L. PEFRYD, *J. Eur. Ceram. Soc.* **7** (1991) 319.
7. M. MAEDA, K. NAKAMURA and T. OHKUBO, *J. Mater. Sci.* **24** (1989) 2120.
8. N. S. JACOBSON, J. L. SMIALEK and D. S. FOX, in "Handbook of Ceramics and Composites, Vol. 1. Synthesis and Properties," edited by N. P. Cheremisinoff (Marcel Dekker, Inc., New York, 1990) p. 99.
9. H. RHO, Ph.D. thesis, University of Dayton, Dayton, Ohio, U.S.A., 1997.
10. M. BACKHAUS-RICOULT and Y. G. GOGOTSI, *J. Mater. Res.* **10**(9) (1995) 2306.
11. F. F. LANGE, *J. Amer. Ceram. Soc.* **61** (1978) C-270.
12. Y. G. GOGOTSI and G. GRATHWOHL, *ibid.* **76**(12) (1994) 3093.

Received 23 February
and accepted 17 November 1999